Two-dimensional solitary waves in media with quadratic and cubic nonlinearity

Ole Bang and Yuri S. Kivshar
Australian Photonics Cooperative Research Center, Research School of Physical Sciences and Engineering, Optical Sciences Centre, Australian National University, Canberra, Australian Capital Territory 0200, Australia

Alexander V. Buryak
School of Mathematics and Statistics, University College, Australian Defence Force Academy, Canberra, Australian Capital Territory 2600, Australia
Optical Sciences Centre, Research School of Physical Sciences and Engineering, Australian National University, Canberra, Australian Capital Territory 0200, Australia

Alfredo De Rossi and Stefano Trillo
Fondazione Ugo Bordoni, Via B. Castaglione 59, 00142 Roma, Italy
(Received 2 February 1998)

We determine the existence and stability regimes of bright $2+1$-dimensional spatial solitary waves in media with quadratic (or $\chi^{(2)}$) and focusing cubic nonlinearities. We derive a necessary criterion for linear stability of these solitons, and use it to show that the quadratic nonlinearity enables stable solitons to exist when the cubic nonlinearity is sufficiently weak. We discuss why the Vakhitov-Kolokolov criterion for stability in $\chi^{(2)}$ systems is only a necessary criterion, and show an example where it fails. We further derive and study a simple adiabatical model for the soliton dynamics close to the instability threshold. Finally, we study the interesting dynamics of the solitons in the unstable regime, where we demonstrate the existence of two different limits described by nonlinear Schrödinger equations. [S1063-651X(98)15409-0]

PACS number(s): 42.65.Tg, 42.60.Jf, 42.65.Jx

I. INTRODUCTION

The basic theory of cascading and two-wave parametric solitons in materials with a pure quadratic (or $\chi^{(2)}$) nonlinearity is now well understood, and importantly, many of the theoretical results have been confirmed experimentally (see [1] for a recent review). In particular, in bulk media as we consider here, families of stable spatial solitons exist above a certain threshold power [2]. Their excitation from input Gaussian beams has been confirmed experimentally [3], as well as numerically without walk off [4] and later with walk off [5]. In fact, it has been shown that self-focusing, leading to a catastrophic collapse, cannot occur in $\chi^{(2)}$ media in any physical dimension [6].

Attention has recently turned to the effect of cubic (or $\chi^{(3)}$) nonlinearity on the known characteristics of solitons and switching in $\chi^{(2)}$ media. The competition between the two types of nonlinearity can, e.g., drastically modify the threshold power for switching [7] and the existence and stability regions of spatial solitary waves diffracting in one transverse dimension (1D) [8–10], and 2D [6,11–13]. It has been shown that the simple model, with only cubic self-modulation and cross-phase modulation (SPM and XPM, respectively) terms added to the known equations for $\chi^{(2)}$ media, does not apply to temporal solitary waves, unless the $\chi^{(2)}$ nonlinearity is much weaker than the $\chi^{(3)}$ nonlinearity [10]. Thus, in contrast to $\chi^{(2)}$ media, spatial and temporal solitary waves do not obey the same dynamical equations in media with competing $\chi^{(2)}$ and $\chi^{(3)}$ nonlinearities. The dependence of the threshold power for collapse on the SPM and XPM coefficients have been investigated [6,12], but in the soliton studies the cubic nonlinearity has so far been assumed to be dispersionless and the ratio of SPM and XPM terms have been fixed. The effect of different SPM to XPM ratios have only recently been investigated [13].

All $\chi^{(2)}$ materials have an *inherent cubic nonlinearity* that becomes important at high powers or when the fundamental wave (FW) and its second harmonic (SH) are not perfectly phase matched. However, this is not the only origin of cubic nonlinearity. When the $\chi^{(2)}$ nonlinearity is periodically varying along the direction of propagation, as in quasi-phase-matched (QPM) media, the effective averaged dynamical equations also include *induced cubic nonlinearities* [14], as a result of incoherent coupling between the wave at the main spatial (QPM) frequency with higher-order modes.

Generally, effective cubic nonlinear terms will appear in the conventional model of $\chi^{(2)}$-induced two-wave mixing due to any kind of incoherent coupling with other modes or higher-order cascading effects. This can be illustrated using the simple example of second-harmonic generation (SHG) in a waveguide, which is single moded at the fundamental frequency ω, but supports two modes at 2ω. The model describing the interaction between the slowly varying envelopes of the modes has the form [15]

$$-i\frac{dA}{dz}=\kappa_1 B_1 A^* e^{-i\Delta k_1 z}+\kappa_2 B_2 A^* e^{-i\Delta k_2 z}, \tag{1}$$

$$-i\frac{dB_n}{dz}=\kappa_n A^2 e^{i\Delta k_n z}, \quad n=1,2, \tag{2}$$

where $A(z)$ and $B_{1,2}(z)$ are the complex amplitudes of the FW and the two SH waves, respectively. The parameter κ_n characterizes the efficiency of the interaction and Δk_n the corresponding phase mismatch. If the coupling to one of the

SH modes, e.g., B_2, is not perfectly matched, we can make the substitution $B_2=\tilde{B}_2\exp(i\Delta k_2 z)$ and use the approximation (cascading limit) $d\tilde{B}_2/dz \ll \Delta k_2 \tilde{B}_2$. From Eq. (2) we then obtain that $\tilde{B}_2 \approx (\kappa_2/\Delta k_2)A^2$, which introduces an effective cubic nonlinearity in Eq. (1),

$$-i\frac{dA}{dz}=\kappa_1 B_1 A^* e^{i\Delta k_1 z}+\frac{\kappa_2^2}{\Delta k_2}|A|^2 A. \tag{3}$$

Incoherent coupling between modes is thus a general physical mechanism that induces cubic nonlinearity.

We note that a similar situation should appear in multistep cascading, when the influence of a third and fourth second-order process, involving both sum and difference frequency mixing, are taken into account [16]. If one of the processes is nearly phase matched, the others can be treated in the cascading limit, leading again to an effective cubic nonlinearity in a way similar to that discussed above for multimoded waveguides.

Since competing quadratic and cubic nonlinearities is a general physical phenomenon, it is important to know the effect of such a competition. In this work we present, to our knowledge for the first time, a complete map of the dynamic properties and existence and stability regimes of the three classes of 2D spatial solitary waves existing in $\chi^{(2)}$ media when inherent focusing cubic nonlinearity is taken into account. The defocusing case was recently considered in [11], whereas the power threshold for collapse in the focusing case was investigated in [6,12].

The paper is organized as follows: In Sec. II we present the dynamical model and compare it with the models used in earlier works on competing nonlinearities. We then consider the case of a bulk medium with focusing dispersionless $\chi^{(3)}$ nonlinearity, and show in Sec. III when the different classes of localized stationary solutions exist, and how their profiles look like.

A mathematical derivation of the Vakhitov-Kolokolov (VK) criterion [17] for linear stability of ground-state bright solitary wave (henceforth soliton) solutions against radially symmetric perturbations is presented in Appendix A, where we also develop a theory that describes their dynamics close to the threshold of instability.

In Sec. IV we use the VK criterion to find the regimes of stability and instability of localized stationary solutions. The power threshold for instability is compared with the analytical predictions of virial theory, which is briefly recapitulated in Appendix B. We further discuss the applicability of the VK stability criterion for such $\chi^{(2)}$ systems, where it is only a *necessary condition,* and present a specific example in which it fails, i.e., predicts stability of solitons that are observed numerically to be unstable.

In Sec. V we look at the specific dynamics in the interesting regimes close to the instability threshold and ''deep'' in the collapse unstable regime. Finally, Sec. VI presents a summary.

II. MODEL

We consider beam propagation in lossless bulk $\chi^{(2)}$ media under conditions for type-I SHG, when cubic material nonlinearity is taken into account. The dynamics is described by the dimensionless equations [10]

$$i\frac{\partial w}{\partial z}+\nabla_\perp^2 w+w^* v+s(|w|^2+\rho|v|^2)w=0, \tag{4}$$

$$2i\frac{\partial v}{\partial z}+\nabla_\perp^2 v-\beta v+\frac{1}{2}w^2+s(\eta|v|^2+\rho|w|^2)v=0, \tag{5}$$

which are valid when spatial walk off is negligible, and both the fundamental frequency ω_1 and its second harmonic $\omega_2=2\omega_1$ are far from resonances. The slowly varying complex envelope function of the FW, $w=w(\vec{r},z)$, and its SH, $v=v(\vec{r},z)$, are assumed to propagate with a constant polarization, $\vec{e}_1$ and $\vec{e}_2$, along the z axis. The transverse Laplacian $\nabla_\perp^2$ refers to the spatial coordinates $\vec{r}=(x,y)$. The electric field $\vec{E}=\vec{E}(\vec{R},Z,T)$ is given by

$$\vec{E}=E_0[we^{i\theta_1}\hat{e}_1+2ve^{i2\theta_1}\hat{e}_2]+\text{c.c.}, \tag{6}$$

in physical coordinates, where $\vec{R}=r_0\vec{r}$, $Z=z_0 z$, and $\theta_1=k_1 Z-\omega_1 T$. The real normalization parameters E_0, z_0, and r_0, are given by (for details see [10])

$$E_0=\frac{4\tilde{\chi}_1^{(2)}}{3|\tilde{\chi}_{1s}^{(3)}|},\quad z_0=2k_1 r_0^2,\quad r_0^2=\frac{3|\tilde{\chi}_{1s}^{(3)}|}{16\mu_0\omega_1^2(\tilde{\chi}_1^{(2)})^2}, \tag{7}$$

where μ_0 is the vacuum permeability and k_n the wave number at the frequency ω_n. The real parameters β, s, η, and ρ are given by [10]

$$\beta=2z_0\Delta k,\quad s=\text{sign}(\tilde{\chi}_{1s}^{(3)}),\quad \eta=\frac{16\tilde{\chi}_{2s}^{(3)}}{\tilde{\chi}_{1s}^{(3)}},\quad \rho=\frac{8\tilde{\chi}_{1c}^{(3)}}{\tilde{\chi}_{1s}^{(3)}}, \tag{8}$$

where $\Delta k=2k_1-k_2 \ll k_1$ is the phase-mismatch parameter, and $\tilde{\chi}_n^{(j)}=\tilde{\chi}^{(j)}(\omega_n)$ denote the Fourier components at frequency ω_n of the jth order susceptibility tensor. Thus $\tilde{\chi}_1^{(2)}=\tilde{\chi}_2^{(2)}$ represents the quadratic nonlinearity, and $\tilde{\chi}_{ns}^{(3)}$ and $\tilde{\chi}_{1c}^{(3)}=\tilde{\chi}_{2c}^{(3)}$ the parts of the cubic nonlinearity responsible for SPM and XPM, respectively. Compared with standard notation these coefficients refer to $\tilde{\chi}_{ns}^{(3)}=\tilde{\chi}^{(3)}(\omega_n=\omega_n-\omega_n+\omega_n)$ and $\tilde{\chi}_{nc}^{(3)}=\tilde{\chi}^{(3)}(\omega_n=\omega_n-\omega_{3-n}+\omega_{3-n})$.

In the form they appear in here, Eqs. (4) and (5) were used to study collapse in media with an arbitrary number of transverse dimensions [6], and to study bright two-dimensional (2D) solitons in the defocusing ($s=-1$) [11] and focusing case ($s=+1$) [12,13]. After a simple transformation they correspond to the 1D equations earlier used in [8,9], and later derived rigorously in [10]. Similar equations were recently shown to describe the dynamics in QPM $\chi^{(2)}$ media [14].

The system (4)–(5) conserves the Hamiltonian H,

$$H=\int\left[|\nabla_\perp w|^2+|\nabla_\perp v|^2+\beta|v|^2-\mathrm{Re}(w^2v^*)\right.$$
$$\left.-\frac{s}{2}(|w|^4+\eta|v|^4+2\rho|wv|^2)\right]d\vec{r}, \tag{9}$$

and the dimensionless power P,

$$P=\int(|w|^2+4|v|^2)d\vec{r}=P_w(z)+4P_v(z), \tag{10}$$

which corresponds to the physical power P_0P, where the normalization parameter $P_0=0.5\sqrt{\epsilon_0/\mu_0}E_0^2r_0^2$ is inverse proportional to $\tilde{\chi}_{1s}^{(3)}$ and independent of $\chi^{(2)}$. Furthermore, Eqs. (4) and (5) are invariant to the phase rotation

$$w\to we^{i\alpha_0},\quad v\to ve^{i2\alpha_0}, \tag{11}$$

and the Galilean transformation

$$w(x,z)\to w(x-2\alpha_1z,z)e^{i\alpha_1(x-\alpha_1z)},$$
$$v(x,z)\to v(x-2\alpha_1z,z)e^{i2\alpha_1(x-\alpha_1z)}, \tag{12}$$

where $\alpha_{0,1}$ are real constants.

Without knowing the experimental setting, and thus the specific values of the $\chi^{(2)}$ and $\chi^{(3)}$ susceptibilities, it is difficult to estimate the values of the dimensionless coefficients η and ρ. However, for a large class of materials and experimental settings, we can neglect the dispersion of $\chi^{(3)}$ and set $\tilde{\chi}_{1s}^{(3)}=\tilde{\chi}_{2s}^{(3)}$, and it is further reasonable to set $\tilde{\chi}_{1s}^{(3)}=\tilde{\chi}_{1c}^{(3)}$. In this case we get $\eta=2\rho=16$, which we use below. These values were also used in earlier works on competing $\chi^{(2)}$ and $\chi^{(3)}$ nonlinearities [8–12]. Furthermore, in this paper we consider only the case of focusing cubic nonlinearity, and thus $s=+1$. For the defocusing case, the existence, stability, and generation of bright solitary waves was analyzed in Ref. [11]. For a recent measurement of the $\chi^{(3)}$ coefficient in several $\chi^{(2)}$ materials we refer to [18].

III. LOCALIZED STATIONARY SOLUTIONS

We consider stationary exponentially localized bright solitary wave solutions (with no nodes, i.e., lowest-order bound states) of the form

$$w(\vec{r},z)=w_0(r)e^{i\lambda z},\quad v(\vec{r},z)=v_0(r)e^{i2\lambda z}, \tag{13}$$

where the real functions w_0 and v_0 tend monotonically to zero as $r=\sqrt{x^2+y^2}$ increases. Inserting this solution into Eqs. (4) and (5), we obtain the stationary equations

$$\nabla_\perp^2w_0-\lambda w_0+w_0v_0+s(w_0^2+\rho v_0^2)w_0=0,$$
$$\nabla_\perp^2v_0-(\beta+4\lambda)v_0+\tfrac{1}{2}w_0^2+s(\eta v_0^2+\rho w_0^2)v_0=0. \tag{14}$$

There are three types of solutions to Eqs. (14) of the form (13): The Combined or C solution, where both components are nonzero, $w_0\neq0$ and $v_0\neq0$, and have no particular relative size. This solution can generally only be found numerically, even for the one-dimensional case (i.e., for $\nabla_\perp^2=d^2/dx^2$)[8,10].

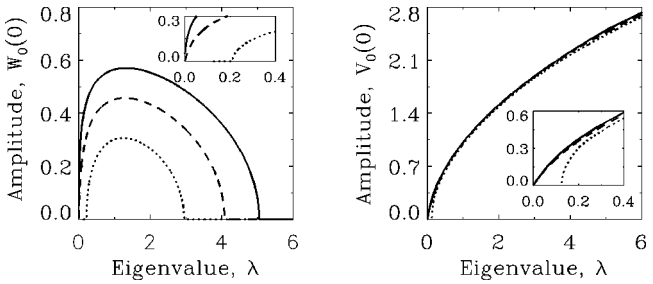

FIG. 1. Amplitude vs λ of (left) the FW and (right) the SH, for the C solutions with $\beta=-0.5$ (dotted), $\beta=0$ (dashed), and $\beta=0.5$ (solid). $\eta=2\rho=16$, $s=+1$.

It is well known that when the effective mismatch is large the cascaded nonlinearity has effective cubic properties. In this limit, where $\beta\gg1$ and $\beta\gg\lambda$, the C solutions asymptotically develop into the single w component or W solution, for which the SH is weak and slaved to the FW, $v_0\approx w_0^2/(2\beta)$. The FW is the solution to the 2D nonlinear Schrödinger (NLS) equation

$$\nabla_\perp^2w_0-\lambda w_0+w_0^3=0, \tag{15}$$

with power $\mathcal{P}_W\simeq P_w=P_{\mathrm{nls}}^c$. Here $P_{\mathrm{nls}}^c=11.69$ is the threshold power for collapse of solutions to the 2D NLS equation (15) [19]. An analytical expression for the solution is not known, but a good approximation can be found by the variational technique to be [20]

$$w_0(r)=A_0\sqrt{\lambda}\ \mathrm{sech}(B_0\sqrt{\lambda}r), \tag{16}$$

where $A_0^2=12\ \ln 2/(4\ln 2-1)$ and $B_0^2=6\ln 2/(2\ln 2+1)$.

In order for C and W solutions (with $w_0\neq0$ and $v_0\neq0$) to be exponentially localized (i.e., have a purely exponential decay in the tails $r\to\infty$), the real propagation constant λ must be above cutoff $\lambda>\lambda_{\mathrm{cut}}\equiv\max\{0,-\beta/4\}$.

The single v component or V solution exists for $\eta>0$. It has no FW, $w_0=0$, and its SH is the solution to the 2D NLS equation

$$\nabla_\perp^2v_0-(\beta+4\lambda)v_0+\eta v_0^3=0, \tag{17}$$

which has the power $\mathcal{P}_V=4P_v=4P_{\mathrm{nls}}^c/\eta$, and is approximately given by

$$v_0(r)=A_0\sqrt{(\beta+4\lambda)/\eta}\ \mathrm{sech}(B_0\sqrt{\beta+4\lambda}r), \tag{18}$$

Since $w_0=0$ the cutoff for the V solution is different from that of the C solution, i.e., $\lambda>-\beta/4$.

Using a standard relaxation technique, we have numerically found the families of C and V solutions for $\lambda>\lambda_{\mathrm{cut}}$. The C family is found starting from the large phase-mismatch limit, using the W solution (16) as a good initial guess. In Fig. 1 we show the amplitudes $w_0(0)$ and $v_0(0)$ of the C solution as function of λ for $\beta=0,\pm0.5$. We see that the C solutions exist only in a certain region, $\lambda_0\leqslant\lambda\leqslant\lambda_1$, which increases with β. For positive β the lower limit is zero, $\lambda_0=0$, while for negative β it is close to, but larger than, the cutoff λ_{cut} (see inserts in Fig. 1 and Fig. 4) and increases with decreasing β. The upper limit λ_1 always increases with β. Thus no C solutions will exist for β less than

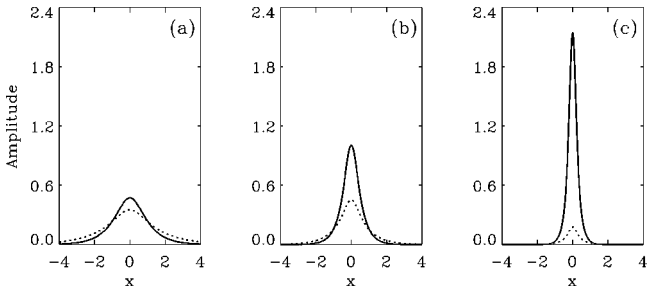

FIG. 2. Profiles $w_0(r=x)$ (dotted) and $v_0(r=x)$ (solid) of the C solutions shown in Fig. 1 for $\beta=0$ and (a) $\lambda=0.3$, (b) $\lambda=1$, and (c) $\lambda=3.8$.

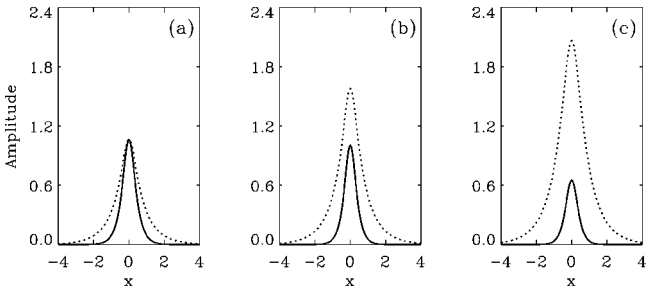

FIG. 3. Profiles $w_0(r=x)$ (dotted) and $v_0(r=x)$ (solid) of the C solutions shown in Fig. 1 for $\lambda=1$ and (a) $\beta=4$, (b) $\beta=10$, and (c) $\beta=20$.

a critical value β_{cr}, which we find to be $\beta_{cr}=-0.914$. The V solutions exist for all values of β and $\lambda>-\beta/4$, and its amplitude is close to the prediction given by Eq. (18). At $\lambda=\lambda_1$ the C solution bifurcates into the V solution. For negative β this also occurs at λ_0.

The profiles of the C solutions are shown in Fig. 2 for $\beta=0$, and three representative values of λ, being in the center of the existence region, and close to the edges $\lambda_0=\lambda_{cut}=0$ and $\lambda_1=4.04$, respectively. We clearly see that the C solution gradually becomes narrower and approaches the V solution with $w_0=0$, as λ increases towards λ_1. Also, as expected, the profile becomes more and more delocalized as the cutoff λ_{cut} is approached.

From Fig. 3 with $\lambda=1$ and $\beta=4$, 10, and 20, we see how the C solution asymptotically develops into the W solution with the SH not just being much weaker, but also much narrower, than the FW. In contrast, as the V solution is approached, the FW and SH seem to have approximately the same width [see Fig. 2(c)].

We have made a series of calculations as shown in Fig. 1, and identified the regions of existence of the different types of localized solutions (13) to Eqs. (14) in the parameter plane (λ,β). The results are summarized in Fig. 4, where we have defined the W solutions as the C solutions in which more than 90% of the power is concentrated in the FW.

We see that the C solutions exist above cutoff, $\lambda>\lambda_{cut}$, when $\beta>\beta_{cr}=-0.914$, while the V solutions always exists above cutoff. As expected, the C solutions develop into the W solutions for $\beta\gg\lambda$. However, it is not necessary that $\beta\gg1$ as assumed in obtaining the W solution (16) theoretically.

IV. STABILITY OF SOLITARY WAVES

A. VK criterion

For conservative systems, under certain conditions, it is possible to derive an analytical criterion for linear stability of solitons, which involves only the dependence of invariants on the solution parameters. A well-known result, first proved by spectral operator theory for a generalized NLS equation, is the Vakhitov-Kolokolov (VK) criterion requiring positive (negative) $dP/d\lambda$ for stability (instability) [17]. The reader is also referred to Ref. [21], where the VK criterion for equations of the NLS type is rigorously proven under a quite general hypothesis, by use of group theory and functional analysis.

In systems with a pure $\chi^{(2)}$ nonlinearity, it has been argued (not proven; see below) that the VK criterion applies to solitons supported by two-wave (or type-I) SHG [22], and three-wave (or type-II) SHG [23], using an adiabatic perturbation technique, and later again for three-wave solitons [24], using spectral operator theory, as originally by Vakhitov and Kolokolov. Here we derive a stability theory for soliton solutions to Eqs. (4) and (5), using the adiabatic perturbation technique first developed for two-wave $\chi^{(2)}$ solitons by Pelinovsky, Buryak, and Kivshar [22] and later for a generalized NLS equation [25], and three-wave $\chi^{(2)}$ solitons [23]. The theory is based on a perturbation expansion around the soliton solution, which is assumed to evolve slowly and adiabatically.

The end result of the mathematical derivation, which is given in Appendix A, is the dynamical equation

$$M(\lambda_0)\frac{d^2\Omega}{dz^2}+P_s'(\lambda_0)\Omega+\tfrac{1}{2}P_s''(\lambda_0)\Omega^2=0, \qquad (19)$$

valid when $|\Omega|\ll1$ and $|P_s'(\lambda_0)|\ll1$. Here $\Omega=\lambda-\lambda_0$, λ_0 is defined by the relation $P_s(\lambda_0)=P$ (for several crossings the one closest to the initial unperturbed soliton value $\lambda(z=0)$ must be chosen), $P_s(\lambda)$ is the soliton power, and prime denotes differentiation with respect to λ. The positive coefficient $M(\lambda)>0$ can be found numerically.

If λ obeys Eq. (19) then an approximate radially symmetric solution exists, whose slow evolution around the initial soliton is described solely by $\lambda(z)$ and the soliton family. Thus, from the linear limit $\Omega^2\approx0$, Eq. (19) predicts that the solitons are stable against radially symmetric perturbations

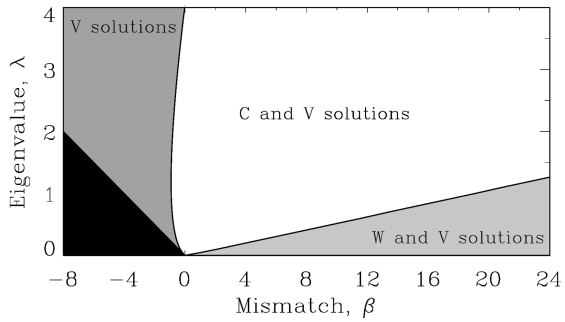

FIG. 4. Regions of existence of C, V, and W solutions in the (λ,β) plane. The W solutions are defined as when 90% of the total power P is in the FW. In the black region $\lambda\leqslant\lambda_{cut}$ and no localized solutions exists. $\eta=2\rho=16$, $s=+1$.

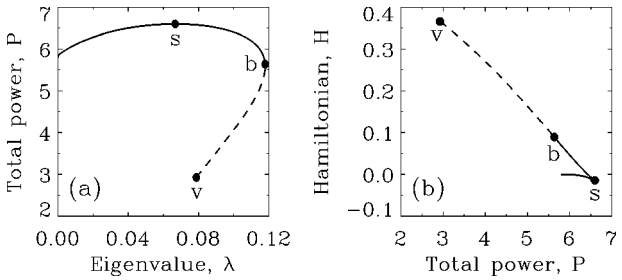

FIG. 5. Soliton bifurcation diagram for $\eta=16$, $\rho=8/3$, and $\beta=0.5$. (a) Power P vs λ. (b) $P-H$ plane. Here b is the bifurcation point between C and C_x solitons, and s is the point where the C solitons change their stability. In the point v the C_x solitons merge with the V solitons.

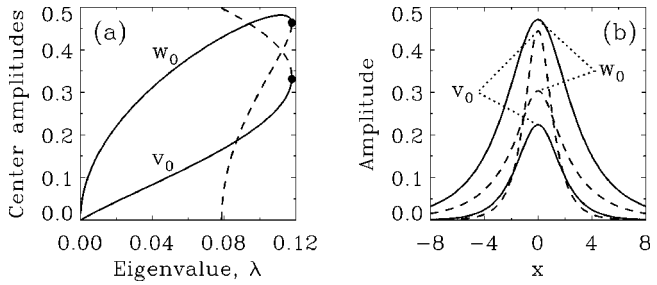

FIG. 6. Soliton amplitudes $w_0(0)$ and $v_0(0)$ (a) and profiles $w_0(r=x)$ and $v_0(r=x)$ at $\lambda=0.1$ (b), for $\eta=16$, $\rho=8/3$, and $\beta=0.5$, as in Fig. 5. Solid lines correspond to C solitons and dashed lines to C_x solitons.

for $P_s'(\lambda_0)>0$ and unstable for $P_s'(\lambda_0)<0$, in agreement with the VK criterion. However, Eq. (19) permits us also to describe the specific dynamics, as long as $|dP_s/d\lambda|\ll 1$ and $|\lambda-\lambda_0|\ll 1$, such as close to the instability threshold. A more general dynamical model, which is valid further away from threshold, but from which a stability criterion cannot be deduced in an analytic form, is also derived in Appendix A. We investigate the dynamics predicted by these models in Sec. V A.

At this point, where the validity of the VK theorem for $\chi^{(2)}$ systems seems well proven, it is appropriate to launch a warning. In all derivations published so far [22–24], as well as the one we give here, the necessary properties of the so-called shift operator $\hat{L}_1$ are simply assumed without a proof. Thus, in the adiabatic perturbation technique (here and [22,23]) it is assumed that $\hat{L}_1$ has only one localized eigenvector with eigenvalue zero (a unique neutral mode), and in the rigorous VK spectral operator theory [24] it is assumed that $\hat{L}_1$ has only one localized eigenvector with negative eigenvalue.

Both properties are proven for the Schrödinger operators of the generalized NLS equation with only one wave component, but not for two-component systems with $\chi^{(2)}$ nonlinearity. This means that the VK stability criterion for $\chi^{(2)}$ systems is only a *necessary* condition, a fact that has not been clearly pointed out in the literature so far. Below we give, for the first time, an example where the VK criterion fails and predicts stability of solitons that are clearly unstable.

Let us consider a representative example with $\eta=16$, $\rho=8/3$, and $\beta=0.5$. In this case, we find the bifurcation diagram shown in Fig. 5. The dashed line represents a new C-soliton family, say C_x, which bifurcates from the ''conventional'' C-soliton family (solid line) at novelty or priority point b ($\lambda_b=0.1178$) and then merges with the V solitons characterized by the λ-independent value $\mathcal{P}_V=2.92$, at point v ($\lambda_v=0.0786$).

The corresponding center amplitudes versus λ, as well as the profiles at $\lambda=0.1$, of the C- and C_x-type solutions, are shown in Fig. 6. Here we see more clearly how the C_x solitons bifurcate from the C solitons and merge with the V solitons with $w_0(x)=0$. In the bifurcation point b the C_x solution is identical to the C solution. From the profiles we see how the C_x soliton has the form (13); i.e., it has no nodes.

Let us now consider stability: According to the VK criterion the C family changes its stability at point s ($\lambda_s=0.066$) where $dP_s/d\lambda$ changes its sign, whereas the C_x family is always stable, having always $dP_s/d\lambda>0$. However, direct numerical simulation shows that the C_x solitons are always unstable. Indeed a numerical analysis reveals that whereas L_1 has only one negative eigenvalue for the C solutions, it has two negative eigenvalues for the C_x solutions. Therefore the VK criterion is correctly applied only for the C family of ground-state solutions, whereas it is meaningless for the C_x family.

In the invariant plane $(P-H)$ the stable C-soliton branch corresponds to the minimum Hamiltonian for a given power, with the C_x family merging with the branch of unstable C solitons. Note, however, that this is not directly related to the assumptions made to prove the VK criterion using spectral operator theory.

The λ interval in which the C_x solution exists becomes narrower as the XPM parameter ρ is increased. For the value $\rho=8$ we use in this work the C_x solution does not exist. However, its appearance for $\rho=8/3$ indicates that the properties of the $\chi^{(2)}+\chi^{(3)}$ system may change significantly when the XPM coefficient is changed. This is supported by the results of Ref. [13].

In the remaining part of the paper we will use the VK stability criterion, but keep in mind that it is only a necessary criterion, and make sure to check several cases by direct numerical simulation before claiming stability.

B. Stability regimes

In Sec. III we showed that at least two types of localized stationary solutions of the form (13) can coexist for given values of the mismatch β and power P: The C and V solutions. Further numerical analysis shows that in general these two solutions do not exist with equal values of the power P, and when they do, the Hamiltonian of the V solution is always larger than that of the C solution (at least for $\eta=2\rho=16$). An example of this is shown in Fig. 7 for $\beta=0$. Consequently, when the two solutions coexist, the V solution is always unstable and the C solution correspond to the ground-state solutions, whose stability properties we will determine in this section using the VK criterion derived in Appendix A.

In Fig. 8 we show the soliton power P versus λ for three values of β. The power of the V solution $\mathcal{P}_V$ is approached as

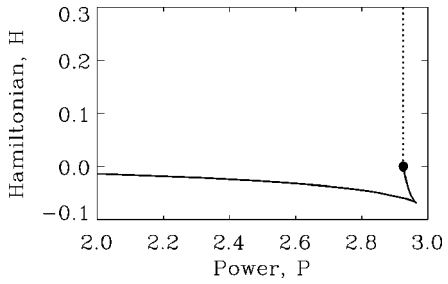

FIG. 7. Hamiltonian H vs total power P for the C solutions (solid) and V solutions (dotted), at $\beta=0$. The two bifurcate into each other at the point marked with a filled circle, corresponding to $\lambda=\lambda_1$ (see Fig. 1). $\eta=2\rho=16$, $s=1$.

λ increases towards the bifurcation point λ_1. Furthermore, for $\beta=-0.5$, the solution is also the V solution for $\lambda_{\rm cut}<\lambda\leqslant\lambda_0$, and therefore the power is also $\mathcal{P}_V$. According to the VK criterion, the solitons are unstable in the whole region of their existence for $\beta=0.5$, whereas a critical value of λ exists at phase matching, $\beta=0$, which separate stable and unstable regions. As the mismatch is further decreased to $\beta=-0.5$, the soliton family exhibits a more complex multistable behavior, the derivative $dP/d\lambda$ changing sign several times.

We have made a series of calculations as shown in Fig. 8, found $dP/d\lambda$, and identified the regions of stability of the soliton solutions in the parameter plane (λ,β). The results are summarized in Fig. 9. We see that the quadratic nonlinearity allows stable bright solitons to exist in bulk media with focusing Kerr nonlinearity, provided the effective mismatch parameter is sufficiently small, $-0.913\leqslant\beta\leqslant0.19$. The possible existence of stable 2D solitons in this model was first predicted from Lyapunov arguments in [6], and is in sharp contrast to purely cubic bulk media described by the 2D NLS equation, in which no stable solutions exist.

In Fig. 10 we show the regions of existence and stability of the soliton solutions in the parameter plane (P,β). Stable solutions are seen to require not only moderate values of the effective mismatch β, but also sufficiently low powers, $P\leqslant3.2$.

It is interesting to compare the results in Fig. 10 with the analytical predictions that can be obtained from the so-called virial theory (see [6] and Appendix B), given by Eqs. (B3) and (B4). A rigorous result of virial theory is that no collapse can occur for powers below $\mathcal{P}_{\rm low}=1.3$ [6]. Our results show that unstable solutions do exist with powers below 1.3 (lower

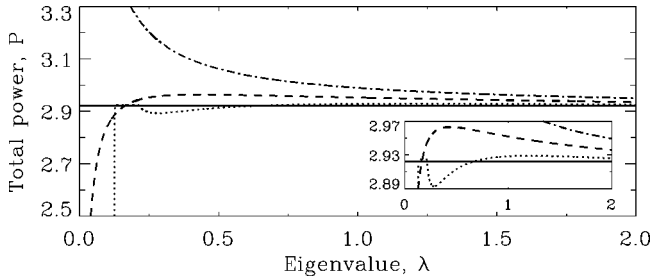

FIG. 8. Power P vs λ for the solutions shown in Fig. 1, with $\beta=-0.5$ (dotted), $\beta=0$ (dashed), and $\beta=0.5$ (dash dotted). The solid line indicates the value $\mathcal{P}_V=2.92$ and the vertical dotted line indicates $\lambda_{\rm cut}=-1/8$.

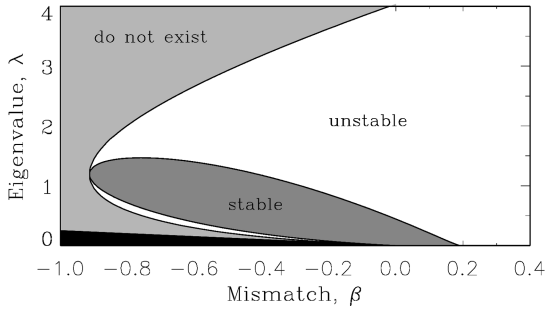

FIG. 9. Regions of existence and stability of solitons in the (λ,β) plane. In the black region $\lambda\leqslant\lambda_{\rm cut}$ and no localized solutions exists. The V solutions exist everywhere else, but are always unstable. $\eta=2\rho=16$, $s=1$.

narrow white region in Fig. 9), but because they are based upon linear stability theory, they do not predict the nature of the instability. However, numerical simulation of Eqs. (4) and (5) have confirmed that the instability is indeed not a collapse instability for $P<1.3$.

Using virial theory one can estimate the threshold power for collapse to be $\mathcal{P}_{\rm high}=3.2$ [6]. This is supported by our calculations, which show that no stable solitons exist for $P>3.2$, corresponding exactly to $\mathcal{P}_{\rm high}$. However, again our results do not show the nature of the instability of the solitons with higher powers, and we have to perform numerical simulations. The results of these (see Fig. 14) confirm that solitons with powers $P>3.2$ indeed collapse after a finite propagation distance.

V. SOLITON DYNAMICS

A. Close to the instability threshold

The adiabatic theory derived in Appendix A allows us to describe the dynamics of the solitons when $|dP_s/d\lambda|\ll1$, such as close to the threshold of instability. Under the action of symmetric perturbations the evolution of the soliton propagation constant λ is then equivalent to that of a single anharmonic oscillator with coordinate λ, momentum $M(\lambda)\dot{\lambda}$, and Hamiltonian energy $\mathcal{H}=\frac{1}{2}M(\lambda)\dot{\lambda}^2+V(\lambda)$, where $V(\lambda)=\int_{\lambda_0}^{\lambda}[P_s(\theta)-P]d\theta$, and the dot denotes differ-

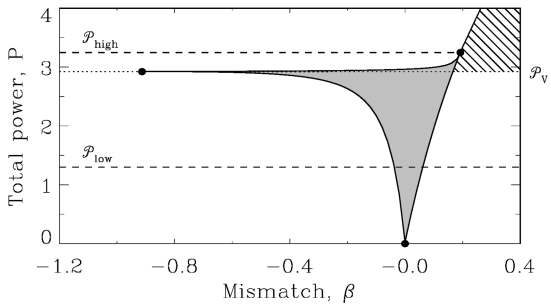

FIG. 10. Existence and stability regions of solitons as a function of the total power P and mismatch β. Stable solitons exist in the shaded region, while unstable solutions exist in both the shaded and hatched regions. The unstable V solutions exist on the dotted line. In the white region no localized solutions of the form (13) exist. The dashed lines indicate the values $\mathcal{P}_{\rm low}=1.3$ and $\mathcal{P}_{\rm high}=3.2$. $\eta=2\rho=16$, $s=1$.

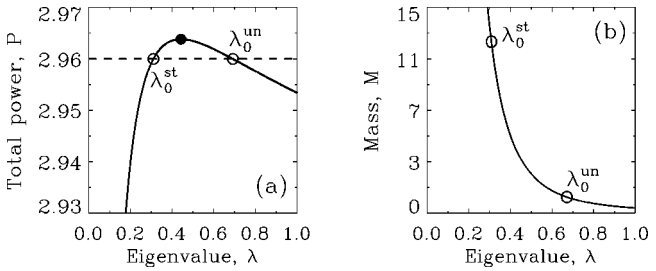

FIG. 11. (a) Power $P_s(\lambda)$ and (b) ''mass'' $M(\lambda)$ for $\beta=0$, $\eta=2\rho=16$, and $s=1$. The instability threshold is marked with a filled circle and the two crossings $\lambda_0^{st}=0.3099$ and $\lambda_0^{un}=0.6918$, with the power $P_s=2.96$ (dashed line), are marked by circles.

entiation with respect to z. Here λ_0 is defined by the relation $P=P_s(\lambda_0)$, where $P_s(\lambda)$ is the power in the unperturbed soliton. If there are several solutions the one closest to the initial unperturbed soliton value $\lambda(z=0)$ must be chosen. The positive ''mass'' $M(\lambda)=2\{\vec{Q},\hat{L}_0\vec{Q}\}$ can be found numerically by solving the equation $\hat{L}_0\vec{Q}=\Theta\partial_\lambda\vec{\psi}^{(0)}$, once the soliton family $\vec{\psi}^{(0)}=[w_0,v_0]^T$ is known.

In Fig. 11 we show the soliton power $P_s(\lambda)$ and the mass $M(\lambda)$ at phase matching $\beta=0$. The total conserved power is $P=2.960$ (dashed line), which is close to the instability threshold, $P_s=2.963$. The two points where $P_s(\lambda)=P$ (circles) correspond to $\lambda=\lambda_0$. Thus λ_0 can have two different values in this case, $\lambda_0^{st}=0.3099$ and $\lambda_0^{un}=0.6918$, at which the mass is $M(\lambda_0^{st})=12.6$ and $M(\lambda_0^{un})=1.1$.

From the VK criterion we know that, to the right of the threshold, where $dP_s/d\lambda$ is negative, the solutions are unstable, and to the left of the threshold, where $dP_s/d\lambda$ is positive, they are stable. The stable and unstable solutions correspond to the lower and upper branches of the curve $H(P)$ (see Fig. 7). However the VK criterion in itself does not give the specific dynamics of the solution.

In Fig. 12 we show the potential $V(\lambda)$ and the corresponding level curves of the oscillator energy $\mathcal{H}$ in the phase plane $\lambda-\dot{\lambda}$, for $\lambda_0=\lambda_0^{un}$ to the right of the threshold (see Fig. 11), where the solution is unstable. From Fig. 12 we see that the points λ_0^{st} and λ_0^{un} correspond to a local minimum and maximum of the potential $V(\lambda)$, respectively, or equivalently to a hyperbolic and elliptic fixpoint in the phase plane $\lambda-\dot{\lambda}$, respectively.

It is clear from the shape of the potential in Fig. 12 that perturbed unstable solitons (moving along level curves in the phase plane) can undergo two qualitatively different types of motion: oscillations (closed curves around the hyperbolic fixpoint) or decay/collapse (open curves) along the direction of growing λ, where the potential is unbounded. Since we know that the soliton solution becomes progressively taller and narrower as λ increases (see Figs. 1 and 2), we expect the latter type of motion to give rise to collapse.

Let us consider an unstable soliton with propagation constant λ_s and power $P_s(\lambda_s)$, under the influence of initial perturbations that are symmetric and real, i.e., $\dot{\lambda}(0)=\alpha_{n0}(0)=0$ (see Appendix A). From Fig. 11 we see that if the perturbation decreases the total power, so that $P<P_s(\lambda_s)$, then $\lambda_s<\lambda_0^{un}$. For such perturbations Fig. 12 shows that the solution will move along a closed orbit, i.e.,

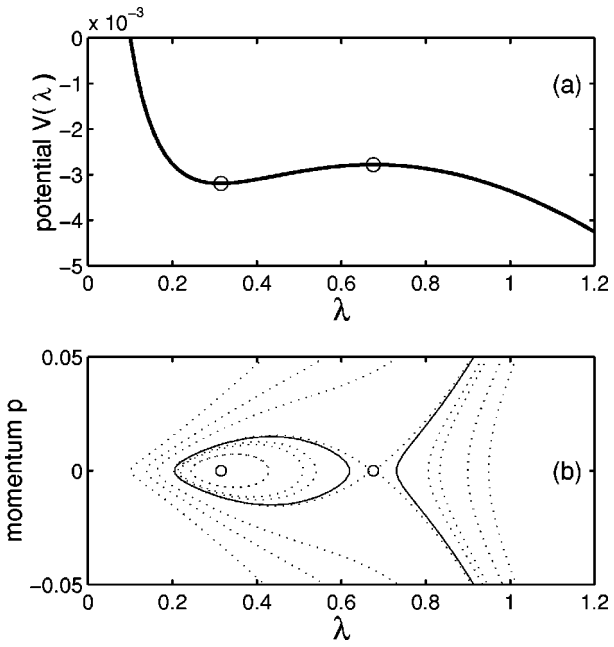

FIG. 12. (a) Potential $V(\lambda)$ for a total power $P=2.96$, and $\lambda_0=\lambda_0^{un}=0.6918$. (b) Level curves of constant $\mathcal{H}$ in the phase-plane $\lambda-p$, where $p=M(\lambda)\dot{\lambda}$. $\beta=0$, $\eta=2\rho=16$, $s=1$.

perform regular oscillations, whose amplitude can be significant. Conversely, if the perturbation increases the total power, so that $P>P_s(\lambda_s)$, then $\lambda_s>\lambda_0^{un}$. For such perturbations Fig. 12 shows that the solution will move in an unbounded potential, i.e., λ should increase indefinitely, eventually causing the solution to collapse.

We verified these predictions by numerically integrating the dynamical Eqs. (4) and (5) with a radially symmetric finite difference scheme. The initial condition is a soliton with power $P_s(\lambda_s)$ modified by multiplying its components ω and θ by $(1+\epsilon)$, where the small perturbation is given by $\epsilon=\sqrt{P/P_s}-1$. In Fig. 13 we show the evolution of an unstable soliton with $\lambda_s=\lambda(0)=0.62<\lambda_0^{un}$ and $P_s(\lambda_s)=2.9609>P$, which is described by the closed orbit shown as a solid line in Fig. 12(b). As predicted we observe a locked (slightly damped) oscillation of the peak amplitudes,

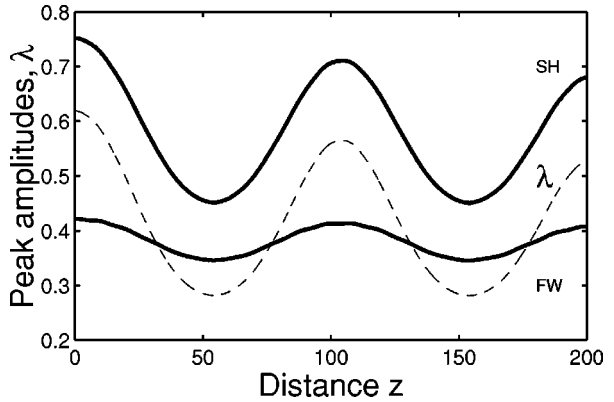

FIG. 13. Numerical simulations of Eqs. (4) and (5), showing the evolution of the center amplitude of the FW and SH (solid), and λ (dashed), for an unstable soliton with $\lambda(0)=0.62$, under the influence of a perturbation that decreases the total power. $\beta=0$, $\eta=2\rho=16$, $s=1$.

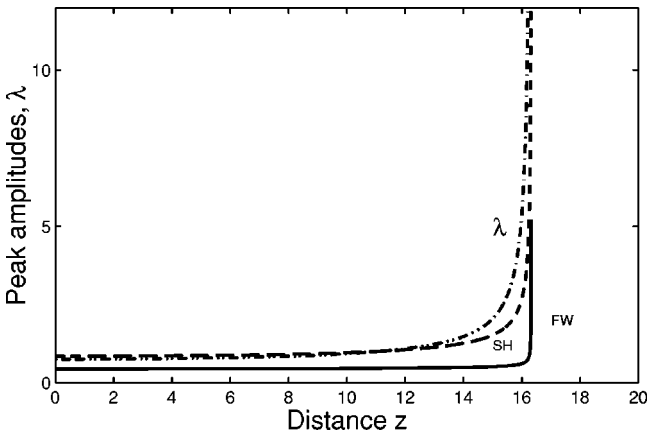

FIG. 14. Numerical simulations of Eqs. (4) and (5), showing the evolution of λ (chain dashed), and the center amplitude of the FW (solid) and SH (dashed), for an unstable soliton with $\lambda(0)=0.75$ and a perturbation that increases the total power $\beta=0$, $\eta=2\rho=16$, $s=1$.

accompanied by a corresponding oscillation of the nonlinear phase shift λ, which we measured as the derivative of the instantaneous phase.

In Fig. 14 we show the evolution of an unstable soliton with $\lambda_s=\lambda(0)=0.75>\lambda_0^{\rm un}$ and $P_s(\lambda_s)=2.9581<P$, which is described by the solid-line open orbit in Fig. 12(b). As predicted the perturbation induces a collapse of both fields at a finite distance.

We note that the oscillations for $\lambda_s=\lambda(0)=0.62<\lambda_0^{\rm un}$ and $P_s(\lambda_s)=2.9609>P$, as observed in Fig. 13, are not described by the expanded potential V_0 and Hamiltonian $\mathcal{H}_0$, given by Eqs. (A26) and (A27), respectively. In this case we get the potential shown in Fig. 15, which clearly predicts either spreading (λ decreases monotonically to zero) or collapse (λ increases monotonically). The reason why the expanded Hamiltonian fails is that the initial value of the propagation constant λ_s is too far from the threshold $\lambda=0.4429$.

B. Collapse in the NLS limits

Even though all solutions in the hatched region in Fig. 10 are (collapse) unstable, this region is nevertheless extremely interesting. In Fig. 16 we show the power versus β, as in Fig. 10, but focusing on the hatched region. The lower limit of

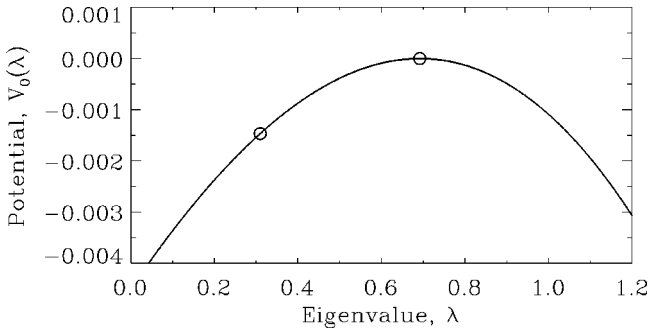

FIG. 15. Expanded potential $V_0(\lambda)$, given by Eq. (A26), for $\lambda_0=\lambda_0^{\rm un}=0.6918$, giving the derivatives $P_s'(\lambda_0^{\rm un})=-0.02169$ and $P_s''(\lambda_0^{\rm un})=-0.01245$. $\beta=0$, $\eta=2\rho=16$, $s=1$.

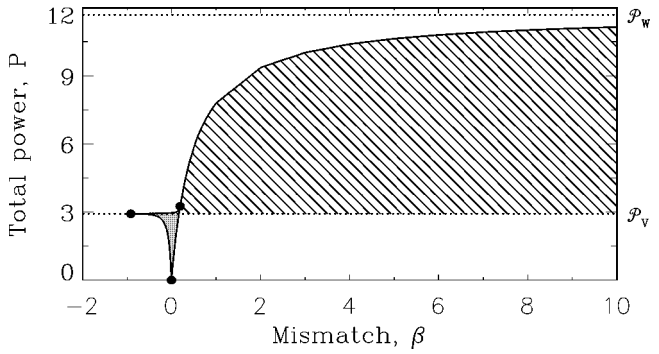

FIG. 16. Power P vs mismatch β as in Fig. 10. The dotted lines indicate $\mathcal{P}_W$ and $\mathcal{P}_V$.

the power in the solutions in this region is always that of the V solution, $\mathcal{P}_V=P_{\rm nls}^{\rm c}/4$, while the upper limit asymptotically approaches that of the W solutions, $\mathcal{P}_W=P_{\rm nls}^{\rm c}$, as β increases.

Thus, in the limit of large phase mismatch, $\beta\gg1$, Eqs. (4) and (5) have collapse unstable solutions with powers in between the two NLS limits, $\mathcal{P}_V\leqslant P\leqslant\mathcal{P}_W$. In the lower limit the FW is zero and the SH is given by the 2D NLS equation (17). In the upper limit, the SH is approximately zero and the FW is given by the 2D NLS equation (15). In contrast, in the (one-field) 2D NLS equation itself, solutions only exist for one value of the power.

One might argue that the ''true NLS limit'' is that of large phase mismatch, where the solution tends to the W solution. It is well known that the $\chi^{(2)}$ nonlinearity has effective cubic properties in this so-called cascading limit (see [1]). However, from the point of view of the solutions to Eqs. (4) and (5), both limits have the characteristic NLS properties.

In Fig. 17 we have depicted P versus λ for several values of $\beta\geqslant1$. Here we clearly see the properties discussed above. Regardless the value of β, the power will always asymptotically decrease towards $\mathcal{P}_V$, as the propagation constant λ increases. At a given point λ_1 the solution will bifurcate into the V solution with the exact power $\mathcal{P}_V$, as we know from Fig. 1. Correspondingly, regardless the value of λ, the power will always increase asymptotically to $\mathcal{P}_W$ as the mismatch β increases. However, there will never be a bifurcation of the solution into the W solution. Finally, we see that the derivative $dP/d\lambda$ tends to zero as either of the NLS limits is approached, in which case the solution is so-called marginally stable, as the solution to the 2D NLS equation [26]. Note that

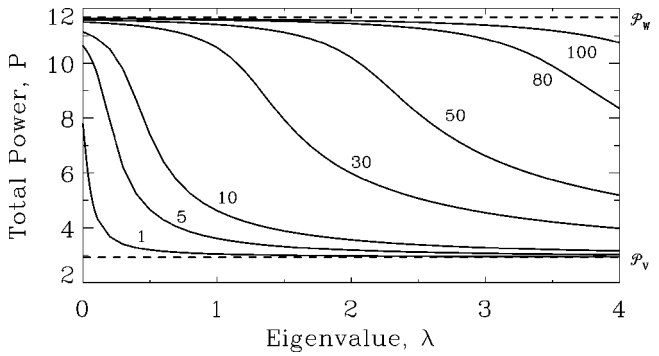

FIG. 17. Power vs λ for different values of β, indicated at the curves. The dotted lines indicate $\mathcal{P}_W$ and $\mathcal{P}_V$.

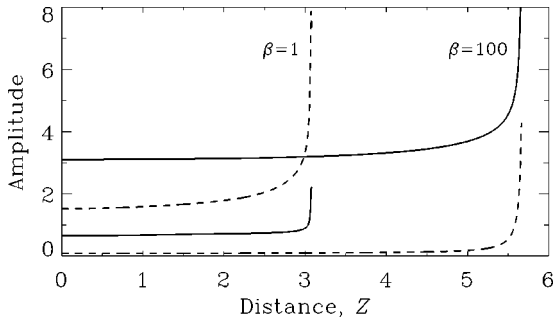

FIG. 18. Evolution of the center amplitudes of the FW (solid) and SH (dashed) for $\lambda=2$, and $\beta=1{,}100$, obtained from numerical simulation of Eqs. (4–5). $\eta=2\rho=16$, $s=1$.

in this limit we could also apply the adiabatic theory to describe the dynamics, as in Sec. V B, since $|dP_s/d\lambda|\ll 1$.

An interesting question regarding the unstable two-component solutions in the hatched region, is which of the fields will initiate the collapse. Physical reasoning says it should be the field with the highest power. To confirm this we show in Fig. 18 the evolution of the center amplitudes of the two fields, as obtained from numerical simulation of Eqs. (4) and (5) for $\lambda=2$. We have not specifically perturbed the solutions, since the perturbations caused by the discretization in the numerical scheme, should be enough to make them collapse [27].

For $\beta=1$ the solution is close to the V solution, and thus the SH dominates over the FW. The specific contribution of the two fields to the total power is $P_w=0.29$ and $4P_v=2.69$. Correspondingly we see that it is the SH that initiates the collapse. For $\beta=100$ the solution is close to the W solution, and thus the FW instead dominates the SH. The specific contribution of the two fields to the total power is now $P_w=11.55$ and $4P_v=0.01$. As expected it is now the FW that initiates the collapse.

An important observation from Fig. 18 is that even though one of the fields is the dominant and initiates the collapse, the other field is ''dragged along'' in the final stage of the collapse. This seems to be a general property, and was also observed in [6].

VI. DISCUSSION

We have analyzed the structure, and existence and stability properties of bright spatial solitary waves propagating in a lossless bulk $\chi^{(2)}$ medium under conditions for type-I SHG, when focusing dispersionless cubic nonlinearity is taken into account. In bulk media with only focusing cubic nonlinearity, such beams are known to always be unstable, i.e., they either diffract or self-focus until a catastrophic collapse, depending on their incident power. In contrast, we have shown that a sufficiently strong quadratic nonlinearity can prevent the catastrophic self-focusing and enable such beams to exist and be stable in media with focusing cubic nonlinearity. The possible existence of such stable 2D solitons was first predicted in [6].

We have found that in order for stable bright spatial solitary waves (henceforth, solitons) to exist the effective phase mismatch β must be sufficiently low, $-0.913\leqslant\beta\leqslant 0.19$, otherwise they will always be unstable. In physical variables (see Sec. II) this corresponds to

$$-1.19<\frac{|x_3|}{x_2^2/\kappa}=1.3\beta<0.25, \tag{20}$$

where $\kappa\equiv n_1^2\Delta k/k_1$, with n_1 being the refractive index at the fundamental frequency, and $x_2=\tilde{\chi}_1^{(2)}/[1\ \mathrm{pm/V}]$ and $x_3=\tilde{\chi}_{1s}^{(3)}/[1\ \mathrm{pm^2/V^2}]$ are the quadratic and cubic nonlinearities, respectively, measured in mks units.

From the relation (20) we see that the cubic nonlinearity, whose strength is proportional to $\tilde{\chi}_{1s}^{(3)}$, must be sufficiently weaker than the quadratic nonlinearity, whose strength is proportional to $[\tilde{\chi}_1^{(2)}]^2/\Delta k$, in order for stable bright spatial solitary waves to exist. Thus even a weak $\chi^{(2)}$ component can arrest self-focusing and enable stable solitons to exist, provided the fundamental and second-harmonic waves are nearly phase matched.

We have shown that when stable bright solitons exist, they always have a dimensionless power P, which is below 3.2. This corresponds to the real physical power

$$P_0P\leqslant 61\ \ \mathrm{kW}\cdot(10^3/|x_3|), \tag{21}$$

for a fundamental wavelength of $\lambda_1=1.3\ \mu$m. Importantly, this power threshold for the existence of stable beams in bulk media with competing quadratic and cubic nonlinearities, is in good agreement with the prediction of the threshold power for collapse, which can be obtained analytically by the so-called virial theory [6], an effective tool for analyzing wave collapse.

We expect the main features discussed above to be found in other systems where a competition between different types of nonlinearities occur. As we have argued, such nonlinear systems are plentiful in optics, since in general any incoherent coupling between two or more waves in multiwave systems, will induce effective higher-order nonlinearities.

In order to study the stability properties of the ground-state solitons we have derived a necessary VK criterion for linear stability, using a perturbation technique based on an assumption of adiabatic evolution of the solitons. This not only gives the VK criterion, but also a model for the dynamics close to the threshold of instability, which predicts two different kinds of instability induced beam evolution: Collapse and regular oscillations of relatively large amplitude. We have confirmed these predictions by numerical simulations.

We have pointed out an obvious mathematical problem with the stability calculations in systems with $\chi^{(2)}$ nonlinearity, based on spectral operator theory, which has not been clearly discussed in the literature so far. For the conventional Schrödinger operators, uniqueness of the neutral modes, in particular, and the oscillator theorem in general, has been rigorously proven. However, this is not the case for $\chi^{(2)}$ and $\chi^{(2)}+\chi^{(3)}$ systems, and not even for coupled NLS equations, where the corresponding operators all become matrix operators.

In particular, the necessary properties of the shift operator have not been proven, such as uniqueness of the neutral mode and existence of only one negative eigenvalue. This means that the VK stability criterion $dP/d\lambda>0$, derived here for $\chi^{(2)}+\chi^{(3)}$ systems, and in Refs. [22–24] for pure $\chi^{(2)}$ systems, is only a necessary condition. To illustrate this we

have given a specific example in which the VK stability theorem fails and predicts stability of solutions that numerical simulations show are unstable.

However, all of the numerical work on bright solitary waves presented so far for pure $\chi^{(2)}$ systems [22–24] supports the hypothesis that $dP/d\lambda>0$ is indeed both a necessary and sufficient criterion for stability of ground-state soliton solutions. In other words, the numerical results support the assumption of the shift-operator of the $\chi^{(2)}$ system having a unique neutral mode and only one negative eigenvalue.

Furthermore, in the limit of a large phase mismatch, the pure $\chi^{(2)}$ system reduces to the NLS equation, whereas the $\chi^{(2)}+\chi^{(3)}$ system reduced to two NLS equations coupled through cross-phase modulation. This strongly suggest that the shift operator of at least the pure $\chi^{(2)}$ system has the same properties as the shift-operator in the NLS equation, i.e., a unique neutral mode and only one negative eigenvalue.

A mathematically rigorous proof of the necessary properties of the $\chi^{(2)}$ and $\chi^{(2)}+\chi^{(3)}$ shift operator, and thus the stability criterion, is still an open problem, and it would be an important issue for future studies.

ACKNOWLEDGMENTS

The authors acknowledge useful discussions with D. Pelinovsky, L. Bergé, E. V. Kuznetsov, J. J. Rasmussen, W. Torruellas, and G. Assanto. Part of this work has been supported by the Australian Department of Industry, Science and Tourism. A. V. Buryak and Yu. S. Kivshar acknowledges the support of the Australian Research Council. The work of S. Trillo was carried out under an agreement with the Istituto Superiore delle Poste e Telecomunicazioni.

APPENDIX A: DERIVATION OF VK CRITERION AND STABILITY THEORY

We consider square- or L^2-integrable functions (finite power or L^2 norm) in a Hilbert space the inner product of which is the L^2 norm

$$\{\vec{a},\vec{b}\}\equiv\int(\vec{a}^{\dagger}\cdot\vec{b})d\vec{r}, \tag{A1}$$

where $\vec{a}^{\dagger}$ denotes the Hermitian conjugate of the vector function $\vec{a}$. Given the inner product, the power can be written as $P=\{\Theta\vec{\Psi},\Theta\vec{\Psi}\}$, where $\vec{\Psi}=[w,v]^T$ and $\Theta=\mathrm{diag}(1,2)$ is a diagonal 2×2 matrix.

The stationary Eqs. (14) have a one parameter family of soliton solutions $\vec{\Psi}=\vec{\psi}^{(0)}(r;\lambda)=[w_0(r;\lambda),v_0(r;\lambda)]^T$. We assume that a certain perturbation leads to a slow and adiabatic evolution of the solitons, determined only by the propagation constant $\lambda=\lambda(Z)$, which now depends on the slow evolution coordinate $Z=\epsilon z$, where $\epsilon\ll1$. Thus we expand the solution as

$$\vec{\Psi}(\vec{r},\lambda)=\exp\left[i\Theta\int_0^z\lambda(\zeta)d\zeta\right]\sum_{n=0}^{\infty}\epsilon^n\vec{\psi}^{(n)}(\vec{r},\lambda), \tag{A2}$$

where $\vec{\psi}^{(0)}$ is real, but the higher-order corrections can be complex. Substituting the expansion (A2) into the dynamical Eqs. (4) and (5) we obtain at the lowest order (ϵ^0) the stationary problem (14). At order ϵ^1 we obtain the inhomogeneous linear problem

$$\hat{L}_0\ \mathrm{Im}\{\vec{\psi}^{(1)}\}=\dot{\lambda}\partial_\lambda\vec{\varphi}_0\equiv\vec{\mathcal{E}}_1, \tag{A3}$$

$$\hat{L}_1\mathrm{Re}\{\vec{\psi}^{(1)}\}=0, \tag{A4}$$

where $\vec{\varphi}_0=\Theta\vec{\psi}^{(0)}$ and dot means derivative with respect to Z. Thus $\vec{\mathcal{E}}_1$ is an even function. The linear 2×2 matrix operators $\hat{L}_n$ are given by

$$\hat{L}_n\equiv\begin{bmatrix}F_n & A_n\\ A_n & G_n\end{bmatrix}, \tag{A5}$$

with the real components

$$F_n=\lambda-\nabla^2+v_0-s(w_0^2+\rho v_0^2)-2n(v_0+sw_0^2),$$

$$G_n=\beta+4\lambda-\nabla^2-s(\eta v_0^2+\rho w_0^2)-2ns\eta v_0^2,$$

$$A_n=-w_0-2ns\rho w_0v_0.$$

The operators $\hat{L}_n$ are real and symmetric, and thus self-adjoint with only real eigenvalues. Furthermore, they are even in $\vec{r}$ (henceforth, just even), i.e., they transform an even function $\vec{F}(\vec{r})=\vec{F}(-\vec{r})$ into an even function $\hat{L}_n\vec{F}(\vec{r})=\hat{L}_n\vec{F}(-\vec{r})$.

The homogeneous equation, $\hat{L}_n\vec{\varphi}=0$, has four linearly independent solutions, which are also eigenfunctions of $\hat{L}_n$ with eigenvalue zero (the so-called neutral modes). The right-hand side (rhs) of Eqs. (A3) and (A4) must be orthogonal to all those homogeneous solutions, which are in the Hilbert space of localized functions that we consider, since $\{\vec{\varphi},\hat{L}_n\vec{u}\}=0$, regardless of the function $\vec{u}$.

For the phase operator $\hat{L}_0$ the real, localized, and even function $\vec{\varphi}_0$ is a homogeneous solution. Let us prove the uniqueness of this neutral mode. For any localized function $\vec{u}=[u_1,u_2]^T$ in the Hilbert space, it is straightforward to show that

$$\{\vec{u},\hat{L}_0\vec{u}\}=\int[w_0^2|\nabla(u_1/w_0)|^2+v_0^2|\nabla(u_2/v_0)|^2$$

$$+(2v_0u_1-w_0u_2)^2/(2v_0)]d\vec{r}\geqslant0, \tag{A6}$$

provided that $\vec{\psi}^{(0)}$ is the ground-state solution, for which $w_0\neq0$ and $v_0\neq0$ for all r and $\lambda(Z)$. For the ground-state solution we can further make the transformation $(u_1,u_2)=(w_0\tilde{u}_1,2v_0\tilde{u}_2)$, since there is a one-to-one correspondence between u_n and $\tilde{u}_n$. From $\{\vec{u},\hat{L}_0\vec{u}\}=0$ we then obtain the relation

$$\int[w_0^2|\nabla\tilde{u}_1|^2+v_0^2|\nabla\tilde{u}_2|^2+2w_0^2v_0(\tilde{u}_1-\tilde{u}_2)^2]d\vec{r}=0.$$

The last term gives that $\tilde{u}_1=\tilde{u}_2$ and the first two give that $\tilde{u}_n(r)$ must be a constant. This proves that the equality sign

in Eq. (A6) applies only to functions that depend linearly on $\vec{\varphi}_0$, and thus $\vec{\varphi}_0$ is the only localized homogeneous solution to Eq. (A3).

To assure orthogonality for all Z between $\vec{\varphi}_0$ and the rhs of Eq. (A3), the unperturbed soliton solutions $\vec{\psi}^{(0)}$ must fulfil the solvability condition $\{\vec{\varphi}_0,\vec{\mathcal{E}}_1\}=0$, which corresponds to $\dot{\lambda}dP_s/d\lambda=0$, where $P_s(\lambda)=\{\vec{\varphi}_0,\vec{\varphi}_0\}$ is the soliton power. In general $\dot{\lambda}\neq 0$ for the solutions we consider, and thus the criterion reduces to $dP_s/d\lambda=0$, which is nothing but the VK threshold condition.

The shift operator $\hat{L}_1$ has the real and odd localized neutral modes $\vec{\varphi}_x=\partial_x\vec{\psi}^{(0)}$ and $\vec{\varphi}_y=\partial_y\vec{\psi}^{(0)}$, and the property that $\hat{L}_1\partial_\lambda\vec{\psi}^{(0)}=-\Theta\vec{\varphi}_0$. We will assume, without a rigorous mathematical proof, that $\vec{\varphi}_x$ and $\vec{\varphi}_y$ are the only neutral modes of $\hat{L}_1$. This means that the stability criterion we derive is only a necessary condition. Since Eq. (A4) is homogeneous equation the orthogonality condition is trivially fulfilled. The criterion $dP_s/d\lambda=0$ is therefore the only solvability condition for Eqs. (A3) and (A4).

Under the condition $dP_s/d\lambda=0$ we can define the vector $\vec{Q}\equiv\vec{L}_0^{-1}\partial_\lambda\vec{\varphi}_0\equiv[q_1,q_2]^T$ in the subspace orthogonal to $\vec{\varphi}_0$, in which $\hat{L}_0$ is invertible, and obtain the first-order correction

$$\vec{\psi}^{(1)}=\alpha_{1x}\vec{\varphi}_x+\alpha_{1y}\vec{\varphi}_y+i[\alpha_{10}\vec{\varphi}_0+\dot{\lambda}\vec{Q}], \tag{A7}$$

where α_{n0}, α_{nx}, and α_{ny} depend on the slow scale Z, with n referring to the order of the correction. The homogeneous part of $\vec{\psi}^{(n)}$ at all orders can be accounted for by the simple transformation

$$\vec{\Psi}(\vec{r},\lambda)\rightarrow\vec{\Psi}(\vec{r}+\epsilon\vec{\Delta},\lambda+\epsilon^2\Omega), \tag{A8}$$

where the corrections are given by

$$\Omega=\dot{\alpha}_{10}+\epsilon\dot{\alpha}_{20}+\cdots,$$

$$\vec{\Delta}=(\alpha_{1x},\alpha_{1y})+\epsilon(\alpha_{2x},\alpha_{2y})+\cdots.$$

It is clear that the odd homogeneous solutions $\vec{\varphi}_{x,y}$ are related to translation, while the even solution $\vec{\varphi}_0$, with the same symmetry as the unperturbed soliton solutions, is related to a change in the propagation constant.

At order ϵ^2 we obtain after some algebra the inhomogeneous linear problem

$$\hat{L}_0\mathrm{Im}\{\vec{\psi}^{(2)}\}=\hat{L}_0\vec{I}_2+\Theta(\dot{\alpha}_{1x}\vec{\varphi}_x+\dot{\alpha}_{1y}\vec{\varphi}_y), \tag{A9}$$

$$\hat{L}_1\mathrm{Re}\{\vec{\psi}^{(2)}\}=\hat{L}_1\vec{J}_2+\vec{\mathcal{E}}_2, \tag{A10}$$

where $\vec{\mathcal{E}}_2$ is even and independent of the homogeneous solutions

$$\vec{\mathcal{E}}_2=-\ddot{\lambda}\Theta\vec{Q}+\dot{\lambda}^2(\vec{R}+\hat{S}\vec{\psi}^{(0)}-\Theta\partial_\lambda\vec{Q}), \tag{A11}$$

with $\vec{R}$ and $\hat{S}$ being given by

$$\vec{R}=\begin{bmatrix} q_1q_2 \\ -q_1^2/2\end{bmatrix},\quad \hat{S}=\begin{bmatrix} s(q_1^2+\rho q_2^2) & 0 \\ 0 & s(\eta q_2^2+\rho q_1^2)\end{bmatrix}.$$

The functions $\vec{I}_2$ and $\vec{J}_2$ are purely a result of the homogeneous solutions, with $\vec{I}_2$ being odd and $\vec{J}_2$ being even. Thus the rhs of Eq. (A9) is odd and trivially orthogonal to the even neutral mode $\vec{\varphi}_0$, and the rhs of Eq. (A10) is even and trivially orthogonal to the odd neutral modes $\vec{\varphi}_{x,y}$. All orthogonality conditions are therefore satisfied at second order.

The contribution from the homogeneous solutions, $\vec{I}_2$ and $\vec{J}_2$, can be accounted for by the redefinition (A8). However, this is not the case for the corresponding contributions proportional to $\dot{\alpha}_{1x}$ and $\dot{\alpha}_{1y}$, unless α_{1x} and α_{1y} are constants, i.e., excluding moving solitons to be taken into account in the straightforward manner indicated by Eq. (A8). In fact, at the next order ϵ^3, there are several homogeneous contributions proportional to α_{1x} and α_{1y}, that cannot be accounted for by the redefinition (A8), unless of course that $\alpha_{1x}=\alpha_{1y}=0$.

In principle the solution to Eqs. (A9) and (A10) could be written down symbolically, as for $\vec{\psi}^{(1)}$ (where $\vec{Q}$ was introduced), and we could proceed to the next order. This would give a set of equations for $\vec{\psi}^{(3)}$, similar to Eqs. (A9) and (A10), but both now including both even and odd components on the rhs, thus imposing a (quite complicated) solvability condition.

We will instead exclude motion and consider only even perturbations, i.e., $\alpha_{nx}=\alpha_{ny}=0$, which simplifies the calculations significantly. In the earlier work [22,23], where this technique was applied, all homogeneous solutions were omitted. Equations (A9) and (A10) now reduce to

$$\hat{L}_0\mathrm{Im}\{\vec{\psi}^{(2)}\}=0,\quad \hat{L}_1\mathrm{Re}\{\vec{\psi}^{(2)}\}=\hat{L}_1\vec{J}_2+\vec{\mathcal{E}}_2, \tag{A12}$$

where $\vec{J}_2=\dot{\alpha}_{10}\partial_\lambda\vec{\psi}^{(0)}-\alpha_{10}\dot{\lambda}\Theta\vec{Q}-\frac{1}{2}\alpha_{10}^2\Theta\vec{\varphi}_0$, and at order ϵ^3 we obtain the inhomogeneous linear problem

$$\hat{L}_0\mathrm{Im}\{\vec{\psi}^{(3)}\}=\hat{L}_0(\vec{I}_3+\ddot{\alpha}_{10}\vec{Q})+\vec{\mathcal{E}}_3, \tag{A13}$$

$$\hat{L}_1\mathrm{Re}\{\vec{\psi}^{(3)}\}=\hat{L}_1\vec{J}_3, \tag{A14}$$

where the even function $\vec{\mathcal{E}}_3$ is given by

$$\vec{\mathcal{E}}_3=\dot{\lambda}[\Theta\partial_\lambda+\hat{T}]\vec{\psi}_p^{(2)}+\dot{\lambda}^3\hat{S}\vec{Q}, \tag{A15}$$

with $\vec{T}$ being defined as

$$\hat{T}=\begin{bmatrix} 2sw_0q_1+q_2 & 2s\rho v_0q_1-q_1 \\ 2s\rho w_0q_2+q_1 & 2s\eta v_0q_2\end{bmatrix},$$

and $\vec{\psi}_p^{(2)}=\hat{L}_1^{-1}\vec{\mathcal{E}}_2$. The functions $\vec{I}_3$ and $\vec{J}_3$ are even, and thus the only solvability condition is $\{\vec{\varphi}_0,\vec{\mathcal{E}}_3\}=0$. Whereas $\vec{I}_3$ and $\vec{J}_3$ can be accounted for by the redefinition (A8), the term proportional to $\ddot{\alpha}_{10}$ cannot.

Straightforward but lengthy calculations show that the equations at order ϵ^4 and ϵ^5 become

$$\epsilon^4:\quad \begin{aligned}&\hat{L}_0\mathrm{Im}\{\vec{\psi}^{(4)}\}=\hat{L}_0(\vec{I}_4+\vec{\mathcal{I}}_4),\\ &\hat{L}_1\mathrm{Re}\{\vec{\psi}^{(4)}\}=\hat{L}_1(\vec{J}_4+\vec{\mathcal{J}}_4)+\vec{\mathcal{E}}_4,\end{aligned}$$

$$\epsilon^5: \quad \begin{array}{c} \hat{L}_0 \mathrm{Im}\{\vec{\psi}^{(5)}\} = \hat{L}_0(\vec{I}_5 + \vec{\mathcal{I}}_5) + \vec{\mathcal{E}}_5, \\ \hat{L}_1 \mathrm{Re}\{\vec{\psi}^{(5)}\} = \hat{L}_1(\vec{J}_5 + \vec{\mathcal{J}}_5), \end{array}$$

where all functions are even, leaving only the one solvability condition $\{\vec{\varphi}_0, \vec{\mathcal{E}}_5\} = 0$. Again $\vec{I}_n$ and $\vec{J}_n$ can be accounted for by the redefinition (A8), whereas $\vec{\mathcal{I}}_n$ and $\vec{\mathcal{J}}_n$ cannot. Thus the homogeneous solutions proportional to α_{n0} and derivatives thereof do not influence the solvability conditions.

The point of the above exercise, keeping the homogeneous contributions as long as possible, is to show that the simple redefinition (A8) cannot account for all the homogeneous contributions. This is only true to a certain order, i.e., to first order for the homogeneous parts associated with displacement (α_{nx} and α_{ny}), and to second order for the part associated with a change in the propagation constant (α_{n0}). Thus one cannot simply omit all homogeneous parts and assume they can be taken into account through Eq. (A8) in the end. In particular, this means that the adiabatic perturbation technique does not allows to easily incorporate odd perturbations that causes the solitons to move transversely.

Our aim is to find an ordinary differential equation for the evolution of the propagation constant $\lambda(Z)$. This can be done in two ways, either by using the combined solvability condition

$$\{\vec{\varphi}_0, \epsilon^1 \vec{\mathcal{E}}_1 + \epsilon^3 \vec{\mathcal{E}}_3 + \epsilon^5 \vec{\mathcal{E}}_5 + \cdots\} = \vec{0}, \tag{A16}$$

or by using the constants of motion and, e.g., inserting the expansion (A2) into the expression for the total power, $P = \{\Theta\vec{\Psi}, \Theta\vec{\Psi}\}$, the z derivative of which should then be zero,

$$\frac{dP}{dz} = \epsilon \frac{d}{dZ}(P_0 + \epsilon^2 P_2 + \epsilon^4 P_4 + \cdots) = 0. \tag{A17}$$

Here we have used that $P_n = 0$ for n odd. The even components are given by

$$P_0 = \{\vec{\varphi}_0, \vec{\varphi}_0\} \equiv P_s,$$

$$P_2 = \{\Theta\vec{\psi}^{(1)}, \Theta\vec{\psi}^{(1)}\} + 2\{\vec{\varphi}_0, \Theta\vec{\psi}^{(2)}\}, \tag{A18}$$

$$P_4 = \{\Theta\vec{\psi}^{(2)}, \Theta\vec{\psi}^{(2)}\} + 2\{\Theta\vec{\psi}^{(1)}, \Theta\vec{\psi}^{(3)}\} + 2\{\vec{\varphi}_0, \Theta\vec{\psi}^{(4)}\}.$$

The two relations (A16) and (A17) are identical, as also pointed out in [25]. Thus it may easily be verified by insertion that $2\{\vec{\varphi}_0, \vec{\mathcal{E}}_n\} = dP_n/dZ = \dot{\lambda} dP_n/d\lambda$.

Since we consider solutions for which $\dot{\lambda} \neq 0$ in general, we obtain from Eq. (A17) the relation

$$P = P_s + \epsilon^2 \left(M\ddot{\lambda} + \frac{M'}{2}\dot{\lambda}^2 \right) + \epsilon^4 P_4 + O(\epsilon^6), \tag{A19}$$

where the coefficient $M(\lambda)$ is given by

$$M(\lambda) = 2\{\vec{Q}, \hat{L}_0\vec{Q}\} = 2\{\partial_\lambda \vec{\varphi}_0, \hat{L}_0^{-1}\partial_\lambda \vec{\varphi}_0\}, \tag{A20}$$

and prime denotes differentiation with respect to λ. From Eq. (A6) we see that $M > 0$ always, since $\vec{Q}$ is orthogonal to $\vec{\varphi}_0$.

Taking only terms of order ϵ^2 or lower into account Eqs. (A19) can be written in the form

$$M\ddot{\lambda} + \frac{M'}{2}\dot{\lambda}^2 + (P_s - P) = 0, \tag{A21}$$

which can be viewed as Hamilton's equations of motion for an effective particle with mass $M(\lambda) > 0$, coordinate λ, and momentum $p = M\dot{\lambda}$, moving in the potential

$$V(\lambda) = \int_{\lambda_0}^{\lambda} [P_s(\theta) - P]\, d\theta, \tag{A22}$$

where λ_0 is defined by the relation $P_s(\lambda_0) = P$ (for several crossings the one closest to the initial unperturbed soliton value $\lambda(z=0)$ must be chosen). The total energy of the particle (or the effective Hamiltonian governing it's dynamics) is given by

$$\mathcal{H}(\lambda, p) = \tfrac{1}{2} M(\lambda)\dot{\lambda}^2 + V(\lambda). \tag{A23}$$

Equation (A21), corresponding to Hamilton's equations $\dot{p} = M\ddot{\lambda} + M'\dot{\lambda}^2 = -\partial\mathcal{H}/\partial q$, for the effective Hamiltonian (A23), thus describes the dynamics of the soliton close to threshold, where $|dP_s/d\lambda| \ll 1$ (see Sec. V). However, it does not provide a criterion for stability in an explicit analytical form.

To derive such an explicit stability criterion we must specify how far λ is from threshold. Inspecting Eqs. (A16)–(A19) we set $\lambda - \lambda_0 = \epsilon^2\Omega$, and assume that $dP_s/d\lambda \sim \epsilon^2$. In this case Eq. (A19) reduces to

$$P = P_s + \epsilon^4 M\ddot{\Omega} + O(\epsilon^6), \tag{A24}$$

since P_4 is proportional to $\dot{\lambda}$. Finally, expanding $P_s(\lambda)$ and $M(\lambda)$ in a Taylor series around λ_0, we obtain to lowest order (ϵ^4) the relation

$$M(\lambda_0)\ddot{\Omega} + P_s'(\lambda_0)\Omega + \tfrac{1}{2}P_s''(\lambda_0)\Omega^2 = 0. \tag{A25}$$

As with Eq. (A19) this relation can be viewed as the equations of motion for an effective particle, now with mass $M(\lambda_0) > 0$, coordinate Ω, and momentum $M(\lambda_0)\dot{\Omega}$, moving in the potential

$$V_0(\Omega) = \tfrac{1}{2}P_s'(\lambda_0)\Omega^2 + \tfrac{1}{6}P_s''(\lambda_0)\Omega^3. \tag{A26}$$

The effective Hamiltonian is now given by

$$\mathcal{H}_0(\Omega, \dot{\Omega}) = \tfrac{1}{2}M(\lambda_0)\dot{\Omega}^2 + V_0(\Omega). \tag{A27}$$

In the linear limit Eq. (A25) permits to identify $P_s'(\lambda_0) > 0$ as a necessary condition for stability and $P_s'(\lambda_0) < 0$ as a sufficient condition for instability against radially symmetric perturbations ($\alpha_{nx} = \alpha_{ny} = 0$), in agreement with the VK criterium.

Equation (A25) gives also a description of the dynamics of the soliton, which is simpler than the one given by Eqs. (A21). However, its regime of validity is more restricted in that it requires the initial soliton to be closer to threshold than is the case for Eq. (A21). An example of this is given in Sec. V.

We note that the VK criterion does only apply to ground-state solutions with no nodes, and not to higher-order solu-

tions with one or more nodes at finite values of r. Even though such higher-order solutions may decay to zero for $r\to\infty$, and thus have finite power, the spectral properties of both the phase and shift operators, $\hat{L}_0$ and $\hat{L}_1$, are not known.

APPENDIX B: VIRIAL THEORY

To obtain predictions about the dynamics we can construct a ''virial'' identity, in analogy with studies of collapse in the NLS equation [26] and the pure $\chi^{(2)}$ system [6]. This consists in the second derivative with respect to z of the virial $R^2(z)$ (for details see [6]):

$$\partial_z^2 R^2 = \frac{4}{P}\left[2(H-\beta P_v)+\mathrm{Re}\left\{\int w^2 v^* d\vec{r}\right\}\right], \qquad \text{(B1)}$$

where $R(z)=[P^{-1}\int r^2(|w|^2+4|v|^2)d\vec{r}]^{1/2}$ is the mean wave radius and $r^2=x^2+y^2$. From Eq. (B1) we see that collapse of the solutions w and v, in the sense $R(z)\to 0$ at a finite z, will take place if the right hand side is negative definite. It was rigorously proven in [6] that if both individual powers are below a given threshold for all z,

$$P_w(z)<P_w^c=\frac{P_{\mathrm{nls}}^c}{1+\rho}, \quad P_v(z)<P_v^c=\frac{P_{\mathrm{nls}}^c}{\lambda+\rho}, \qquad \text{(B2)}$$

then such a collapse can never occur. To assure that Eq. (B2) is satisfied for all z the total power must be sufficiently low,

$$P<\mathcal{P}_{\mathrm{low}}=\min\{P_w^c,4P_v^c\}. \qquad \text{(B3)}$$

Furthermore, we can estimate that collapse should possibly occur if the total power is sufficiently high,

$$P>\mathcal{P}_{\mathrm{high}}\equiv P_w^c+4P_v^c, \qquad \text{(B4)}$$

under the additional requirement $H<0$. We stress that the limit (B3) is a rigorous result, while Eq. (B4) is only an estimate based on a comparison with pure $\chi^{(3)}$ media [6]. In the intermediate range $\mathcal{P}_{\mathrm{low}}<P<\mathcal{P}_{\mathrm{high}}$ nothing definite can be concluded from the virial identity.

These predictions were tested numerically for $\beta=0$ and positive values of λ and ρ, which verified the lower bound (B3), and showed that the upper bound (B4) was reliable, except for a narrow region of the parameter space, where it was slightly underestimated [6,12]. In the particular case $\eta=2\rho=16$, it was shown numerically in [12], that $\mathcal{P}_{\mathrm{high}}$ is a reasonable estimate of the actual threshold power for moderate values of β, i.e., $|\beta|\leqslant 4$.

[1] G. I. Stegeman, D. J. Hagan, and L. Torner, Opt. Quantum Electron. **28**, 1691 (1996).

[2] A. A. Kanashov and A. M. Rubenshik, Physica D **4**, 122 (1981). K. Hayata and M. Koshiba, Phys. Rev. Lett. **71**, 3275 (1993); V. V. Steblina, Yu. S. Kivshar, M. Lisak, and B. A. Malomed, Opt. Commun. **118**, 345 (1995); A. V. Buryak, Yu. S. Kivshar, and V. V. Steblina, Phys. Rev. A **52**, 1670 (1995); L. Torner, D. Mihalache, D. Mazilu, E. M. Wright, W. Torruellas, and G. I. Stegeman, Opt. Commun. **121**, 149 (1995).

[3] W. E. Torruellas, Z. Wang, D. E. Hagan, E. W. Van Stryland, G. I. Stegeman, L. Torner, and C. R. Menyuk, Phys. Rev. Lett. **74**, 5036 (1995); R. A. Furst, B. L. Lawrence, W. E. Torruellas, and G. I. Stegeman, Opt. Lett. **22**, 19 (1997).

[4] L. Torner, C. R. Menyuk, W. E. Torruellas, and G. I. Stegeman, Opt. Lett. **20**, 13 (1995).

[5] L. Torner and E. M. Wright, J. Opt. Soc. Am. B **13**, 864 (1996); G. Leo, G. Assanto, and W. Torruellas, *ibid.* **14**, 3134 (1997).

[6] L. Bergé, O. Bang, J. J. Rasmussen, and V. K. Mezentsev, Phys. Rev. E **55**, 3555 (1997).

[7] A. Kobyakov, F. Lederer, O. Bang, and Yu. S. Kivshar, Opt. Lett. **23**, 506 (1998).

[8] A. V. Buryak, Y. S. Kivshar, and S. Trillo, Opt. Lett. **20**, 1961 (1995); S. Trillo, A. V. Buryak, and Y. S. Kivshar, Opt. Commun. **122**, 200 (1996).

[9] M. A. Karpierz, Opt. Lett. **20**, 1677 (1995).

[10] O. Bang, J. Opt. Soc. Am. B **14**, 51 (1997).

[11] O. Bang, Yu. S. Kivshar, and A. V. Buryak, Opt. Lett. **22**, 1680 (1997).

[12] O. Bang, L. Bergé, and J. J. Rasmussen, Opt. Commun. **146**, 231 (1998).

[13] A. De Rossi, G. Assanto, S. Trillo, and W. Torruellas, Opt. Commun. **150**, 390 (1998).

[14] C. B. Clausen, O. Bang, and Yu. S. Kivshar, Phys. Rev. Lett. **78**, 4749 (1997).

[15] C. G. Treviño-Palacios, G. I. Stegeman, M. P. De Micheli, P. Baldi, S. Nouh, D. B. Ostrowsky, D. Delacout, and M. Papuchon, Appl. Phys. Lett. **67**, 170 (1995).

[16] K. Koynov and S. Saltiel, Opt. Commun. **152**, 96 (1998).

[17] M. G. Vakhitov and A. A. Kolokolov, Radiophys. Quantum Electron. **16**, 783 (1975).

[18] H. Li, F. Zhou, X. Zhang, and W. Ji, Opt. Commun. **144**, 75 (1997).

[19] N. E. Kosmatov, V. F. Shvets, and V. E. Zakharov, Physica D **52**, 16 (1991).

[20] D. Anderson, M. Bonnedal, and M. Lisak, Phys. Fluids **22**, 1838 (1979).

[21] M. Grillakis, J. Shatah, and W. Strauss, J. Funct. Anal. **74**, 160 (1987).

[22] D. E. Pelinovsky, A. V. Buryak, and Yu. S. Kivshar, Phys. Rev. Lett. **75**, 591 (1995).

[23] A. V. Buryak, Yu. S. Kivshar, and S. Trillo, Phys. Rev. Lett. **77**, 5210 (1996).

[24] Y. Chen, Phys. Lett. A **234**, 443 (1997).

[25] D. E. Pelinovsky, V. V. Afanasjev, and Yu. S. Kivshar, Phys. Rev. E **53**, 1940 (1996).

[26] J. J. Rasmussen and K. Rypdal, Phys. Scr. **33**, 481 (1986).

[27] O. Bang, J. J. Rasmussen, and P. L. Christiansen, Nonlinearity **7**, 205 (1994).